



Optimization of sol–gel spin-coated $\text{Cu}_2\text{ZnSnS}_4$ (CZTS) thin-film control parameters by RSM method to enhance the solar cell performance

Siddhant B. Patel¹ and Jignasa V. Gohel^{1,*}

¹Department of Chemical Engineering, Sardar Vallabhbhai National Institute of Technology, Surat, Gujarat 395 007, India

Received: 8 February 2018

Accepted: 15 May 2018

Published online:
31 May 2018

© Springer Science+Business
Media, LLC, part of Springer
Nature 2018

ABSTRACT

This present study aims to investigate a specific optimum deposition condition for the synthesis of $\text{Cu}_2\text{ZnSnS}_4$ (CZTS) thin films by a sol–gel spin-coating method. Spin speed (X_1), spin time (X_2), annealing temperature (X_3) and annealing time (X_4) are considered as the major control parameters (independent variables). Response surface methodology technique is implemented for the first time to optimize multiple responses (dependent variable) for sol–gel spin-coated CZTS thin films. Band gap and power conversion efficiency (PCE) are considered as the responses. All the independent variables are varied at three different levels. The Box–Behnken design (BBD) array is opted for the optimization, as it gives optimized results for more than three parameters in less number of experiments. Four control variables and three levels involve 81 experiments to find out optimum deposition condition, whereas BBD can achieve more specific optimum condition in only 29 experiments. Furthermore, mathematical models for band gap and PCE are established as the function of control parameters. Additionally, the influence of the control parameters on both responses is investigated by ANOVA results of models. By the optimization of models, a specific optimum deposition condition $X_1 = 2104$ rpm, $X_2 = 38$ s, $X_3 = 527$ °C and $X_4 = 68$ min is achieved. 1.51 eV band gap and 3.53% PCE are predicted for the optimum condition. Moreover, a validation experiment is carried out at nearest integer value: $X_1 = 2100$ rpm, $X_2 = 38$ s, $X_3 = 530$ °C and $X_4 = 68$ min. 1.50 eV band gap and 3.55% PCE are achieved as the results, which is in good agreement with predicted results. The optimum condition leads to 17.55% of enhancement in PCE than PCE achieved without optimization.

Address correspondence to E-mail: jignasa.narsinhbhai@gmail.com; sjn@ched.svnit.ac.in

Introduction

In the perspective of environmental issues and the fast diminishing conventional energy sources, renewable energy demand is exponentially increasing. It has encouraged rigorous research for the novel, more efficient, and green energy sources with advanced technology [1]. Hence, the solar energy is receiving a considerable attention of scientific community attributed to the availability of unlimited energy from the sun [2]. Photovoltaic cells are excellent option for the energy supply in the remote and domestic area. At present, the photovoltaic market is mainly covered by silicon-based solar cells [3]. However, the silicon-based solar cells are expensive owing to the high cost of pure silicon as well as the cell preparation method [4]. Hence, thin-film solar cells are introduced. In the beginning, CIGS (copper indium gallium selenide) and CdTe (cadmium telluride)-based thin-film solar cells were introduced [5]. However, production of these solar cells on the commercial scale is restricted due to less availability of In and Te and toxicity of Cd and Se [6]. Thus, to overcome these issues, copper zinc tin sulfide (CZTS)-based solar cells are introduced [7].

Up till now, numerous researches on CZTS thin-film preparation by different deposition techniques have been reported such as thermal deposition [8], pulsed laser deposition [9], electrodeposition [10], spray pyrolysis [11] and sol-gel spin coating [12]. Amid these techniques, the sol-gel spin coating is simplest and most efficient low-cost thin-film preparation technique. It is well known that the CZTS is a quaternary substance [13]. Hence, synthesis of single-phase CZTS thin film is quite challenging. For the synthesis of a single-phase CZTS thin film, it is necessary to know the thin-film control parameters. So far, the major studies have considered one factor/control parameter at a time for the CZTS thin-film properties optimization. Yu et al. [14] and Wu et al. [13] studied the effect of spin speed on the properties of CZTS thin films. The effect of annealing temperature on optical properties of CZTS thin films is also well reported [16–18]. Tchognia et al. [19] investigated the effect of annealing time on the properties of CZTS thin films. Nevertheless, multiple parameter consideration for optimization is very scarcely reported. Tchognia et al. [20] reported multiple parameter optimization for only single response

(band gap) by Taguchi approach. However, no validation test was carried out to validate the findings. Moreover, Taguchi approach can optimize only one response at a time and gives an optimum combination of the control parameters, not a specific condition [21]. Hence, to achieve a specific optimum condition and carry out multi-response optimization response surface methodology (RSM) must be implemented [22]. To the best of author's knowledge, a comprehensive study on the simultaneous effect of each of the major parameters on the multiple responses (band gap and PCE) for optimization of sol-gel spin-coated CZTS thin film by RSM is not yet reported. Hence, there is a need for such comprehensive study.

In the present study, CZTS thin films are prepared by the sol-gel spin-coating technique. The four major thin-film control parameters, namely spin speed, spin time, annealing temperature and annealing time, are considered based on the literature available and our previous parametric study [23, 24]. All the parameters are varied at three different levels. RSM, the Box-Behnken design, is implemented for the optimization of control parameters in terms of multiple responses. The band gap and power conversion efficiency (PCE) are considered as the responses. Design Expert software is implemented to generate mathematical model between control parameters and responses. The analysis of model is also carried out with the help of software. Further, the effect of the control parameter on both band gap and PCE is obtained by analysis of variance (ANOVA) results. In addition, optimization of mathematical model is carried out and a specific optimum deposition condition is acquired. A validation test is also carried out to confirm whether the obtained specific optimized condition leads to maximum PCE or not.

Experimental

FTO pretreatment

The FTO (fluorine-doped tin oxide, $\sim 7\Omega/\text{sq.}$) glass substrate was purchased from Sigma-Aldrich. FTO substrate was properly cleaned as per the method described in our previous study [11]. Substrate was first etched with Zn powder and diluted HCl and then rinsed with DI water. Further, it was sonicated with acetone, followed by rinsing with DI water, and finally dried under vacuum oven.

CZTS thin-film preparation

The CZTS thin films were synthesized by a very cost-effective sol-gel spin-coating technique. The sol-gel solution was prepared by dissolving copper chloride, zinc acetate, tin chloride and thiourea into propylene glycol. All the chemicals were purchased from Finar Ltd., India. Few drops of MEA (monoethanolamine) were added as a stabilizer. A clear yellow-colored solution was obtained at the end of 1 h stirring at room temperature. Further, the solution was spin-coated using spin coater (VB Ceramic Consultants, Chennai, India) on the cleaned FTO substrate. Subsequently, the film was dried at 230 °C temperature. The deposition process was carried out 7 times in order to acquire desired film thickness (1–2 μm). Lastly, the film was annealed under argon atmosphere. The spin speed, spin time, annealing temperature and annealing time were varied at three different levels (low level, medium level and high level), which are listed in Table 1 (in “Design of experiments and analysis” section). All the experiments were carried out as per Box–Behnken design array shown in Table 2 (in “Design of experiments and analysis” section).

Device fabrication

Furthermore, to obtain PCE (second response), the solar cell devices were prepared and analyzed. The device was fabricated using the thin film prepared at each array of Box–Behnken design and optimum thin film as well. In the previous studies, the solar cell was fabricated as FTO/i-ZnO/Al:ZnO/CdS/CZTS/CuS/FTO in order to cover full light spectra [23]. The similar solar cell was fabricated in the present study, to compare the PCE with PCE that of previously reported (3.02%) [23]. i-ZnO (intrinsic ZnO) layer was deposited by spray pyrolysis method as previously reported [25]. The doping in ZnO was optimized in our previous studies [26, 27]. Consequently, the Al-doped ZnO layer was deposited upon i-ZnO layer using same deposition condition. Subsequently, the

CdS layer was deposited on the Al:ZnO layer by the spin-coating method. Further, on the CdS layer, CZTS film was deposited as per Box–Behnken design array mentioned in Table 2 in “Design of experiments and analysis” section and optimum condition achieved after optimization as well. Lastly, a counter electrode of CuS/FTO was prepared by depositing CuS solution on another FTO by spray pyrolysis method.

Design of experiments and analysis

In the present study, response surface methodology (RSM) technique was implemented to obtain a specific optimum deposition condition. Box and Draper first introduced response surface methodology in 1987 as the optimization tool [28]. The response surface methodology uses the mathematical and statistical techniques to develop a mathematical relationship between the desired response and associated control parameters [29]. Typically, this relationship is unknown but can be derived by a low-order polynomial regression model. The regression model can be derived from the orthogonal array design of experiments. Basically, RSM follows two designs, namely central composite design (CCD) and Box–Behnken design (BBD) [30]. In the present study, BBD was selected owing to its advantage of less number of experiments over CCD. In the present study, four major control parameters and three different levels of each parameter led to 29 experiments in BBD. Table 1 illustrates the control parameters and their three different level values. The range of parameter was decided based on the literature and our previous parametric study [14, 15, 31–33]. Table 2 depicts the experimental design of BBD array.

The regression analysis of the experimental data was carried out using the following polynomial model, given as Eq. (1).

$$Y = \beta_0 + \sum_{i=1}^k \beta_i X_i + \sum_{i=1}^k \beta_{ii} X_i^2 + \sum_{i < j}^k \sum \beta_{ij} X_i X_j + \varepsilon \quad (1)$$

Table 1 The independent control parameters and their coded levels for thin-film preparation

Control parameters (Factors)	Symbol	Low level (− 1)	Medium level (0)	High level (1)
Spin speed (rpm)	X_1	1000	2000	3000
Spin time (s)	X_2	20	40	60
Annealing temp (°C)	X_3	450	500	550
Annealing time (min)	X_4	30	60	90

Table 2 Box–Behnken design array for four factors and three levels along with experimental data of responses, band gap (Y_1) and PCE (Y_2)

Std. order	Factors				Responses	
	X_1 (rpm)	X_2 (s)	X_3 (°C)	X_4 (min)	Y_1 (eV)	Y_2 (%)
1	1000	20	500	60	1.66	2.8
2	3000	20	500	60	1.63	2.95
3	1000	60	500	60	1.68	2.7
4	3000	60	500	60	1.65	2.85
5	2000	40	450	30	1.87	1.75
6	2000	40	550	30	1.61	3.05
7	2000	40	450	90	1.82	2
8	2000	40	550	90	1.56	3.3
9	1000	40	500	30	1.7	2.6
10	3000	40	500	30	1.66	2.8
11	1000	40	500	90	1.65	2.85
12	3000	40	500	90	1.63	2.95
13	2000	20	450	60	1.8	2.1
14	2000	60	450	60	1.86	1.8
15	2000	20	550	60	1.56	3.25
16	2000	60	550	60	1.58	3.15
17	1000	40	450	60	1.88	1.7
18	3000	40	450	60	1.85	1.85
19	1000	40	550	60	1.62	2.95
20	3000	40	550	60	1.59	3.1
21	2000	20	500	30	1.66	2.75
22	2000	60	500	30	1.67	2.72
23	2000	20	500	90	1.6	3.1
24	2000	60	500	90	1.62	3
25	2000	40	500	60	1.54	3.4
26	2000	40	500	60	1.56	3.3
27	2000	40	500	60	1.55	3.35
28	2000	40	500	60	1.54	3.35
29	2000	40	500	60	1.56	3.3

Y_1 Band gap of CZTS thin films (eV), Y_2 PCE of CZTS thin-film solar cells (%)

where Y = desired response, $\beta_1, \beta_2, \dots, \beta_k$ = regression coefficient of linear effect, $\beta_{11}, \beta_{22}, \dots, \beta_{ii}$ = regression coefficient of quadratic effect, $\beta_{12}, \beta_{13}, \dots, \beta_{ij}$ = regression coefficient of interaction effect, ε = error, X_1, X_2, \dots, X_k = control variables (factors). Here, $k = 4$ as four independent control parameters were considered. The empirical mathematical relationship between the control parameters (independent variables) and the desired response (dependent variables) was obtained by analyzing above regression model. Further, Design Expert V10 software was employed to carry out the statistical analysis. Analysis of variance (ANOVA) was carried out to check the competence of the developed mathematical equation. R^2 value, F-test and lack-of-fit test were employed to determine the significance and

acceptability of the model. Response surface plots were drawn to study the effects of independent parameters on the desired responses.

Characterization

The structural properties of the CZTS films were investigated by X-ray diffraction (XRD, Rigaku D/Max 2200). The analysis was carried out in 10 to 90° 2θ range at 0.02° scanning rate. The optical properties were studied by UV–visible (HACH-DR 6000) spectroscopy. The Tauc's plot method was employed to determine the band gap of CZTS thin film. The surface morphological analysis was carried by scanning electron microscope (SEM) S3400, Hitachi International Ltd., and instrument was used to

perform the SEM analysis. The solar cell performance was measured by SS150 AAA solar simulator (Science Tech., USA) along with Keithley 2400 (Keithley Instruments, Inc, USA) source meter. The solar cell performance measured under the 100 mW/cm² illumination. As a source of light, xenon lamp was used.

Results and discussion

Regression model

Optimization of the thin-film control parameters was carried out with BBD in order to identify the optimum deposition conditions for the sol-gel spin-coated CZTS thin films. The experimental design of

Table 3 Model adequacy summary for both response band gap and PCE

Source	SS	DF	MS	F value	p value	Remarks
<i>Sequential model sum of squares for band gap</i>						
Mean	79.97881	1	79.97881			
Linear	0.214383	4	0.053596	12.25014	< 0.0001	
2FI	0.000525	6	8.75E-05	0.015075	1.0000	
Quadratic	0.103436	4	0.025859	347.5457	< 0.0001	Suggested
Cubic	0.000467	8	5.83E-05	0.608696	0.7480	Aliased
Residual	0.000575	6	9.58E-05			
Total	80.2982	29	2.768903			
<i>Sequential model sum of squares for PCE</i>						
Mean	224.9584	1	224.9584			
Linear	5.120317	4	1.280079	11.49682	< 0.0001	
2FI	0.013725	6	0.002288	0.015488	1.0000	
Quadratic	2.626191	4	0.656548	284.6452	< 0.0001	Suggested
Cubic	0.018133	8	0.002267	0.960565	0.5350	Aliased
Residual	0.014158	6	0.00236			
Total	232.7509	29	8.025893			
<i>Lack-of-fit tests for band gap</i>						
Linear	0.104603	20	0.00523	52.30144	0.0008	
2FI	0.104078	14	0.007434	74.34134	0.0004	
Quadratic	0.000642	10	6.42E-05	0.641667	0.7410	Suggested
Cubic	0.000175	2	8.75E-05	0.875	0.4839	Aliased
Pure error	0.0004	4	0.0001			
<i>Lack-of-fit tests for PCE</i>						
Linear	2.665207	20	0.13326	76.14878	0.0004	
2FI	2.651482	14	0.189392	108.2238	0.0002	
Quadratic	0.025292	10	0.002529	1.445238	0.3858	Suggested
Cubic	0.007158	2	0.003579	2.045238	0.2444	Aliased
Pure error	0.007	4	0.00175			
Source	SD	R ²	Adjusted R ²	Predicted R ²	PRESS	
<i>Model summary statistics for band gap</i>						
Linear	0.066145	0.671235	0.616441	0.580255	0.134061	
2FI	0.076186	0.672879	0.491145	0.347871	0.208281	
Quadratic	0.008626	0.996739	0.993477	0.986471	0.004321	Suggested
Cubic	0.009789	0.9982	0.991598	0.919142	0.025825	Aliased
<i>Model summary statistics for PCE</i>						
Linear	0.333679	0.657081	0.599927	0.560722	3.423084	
2FI	0.384309	0.658842	0.46931	0.313307	5.35107	
Quadratic	0.048027	0.995856	0.991712	0.979902	0.156618	Suggested
Cubic	0.048577	0.998183	0.991521	0.866316	1.041738	Aliased

SS sum of square, DF degree of freedom, MS mean square

BBD along with its results of both the responses is illustrated in Table 2. Further, the results are analyzed by the Design Expert V10 software. In the present study, all the possible mathematical models were fitted to the obtained data using the software. The fitting summary of all the models for both the responses is depicted in Table 3.

The significance of the model is decided on the basis of the p value. Lowest p value suggests the high significance of the model or better fitting model. In addition, R^2 value (should be closer to 99%), F value (should be high), p value associated with lack-of-fit error (should be high) and PRESS value (should be lower) are also considered to adopt the best suitable model. Based on data in Table 3, the lowest p value (< 0.0001), high R^2 value (99.67%), high F value (347.55), high p value for lack of fit (0.7410) and lowest PRESS value (0.00043) are observed for the quadratic model in the case of band gap. Similarly, in the case of PCE, lowest p value (< 0.0001), high R^2 value (99.59%), high F value (284.65), high p value for lack of fit (0.3858) and lowest PRESS value (0.16) are observed for the quadratic model. Hence, it can be concluded that the second-order polynomial (quadratic) model is appropriately fitting in the present case (with both the responses). By analyzing data of Table 2, following second-order quadratic equations (Eqs. 2, 3) are acquired for both the responses from the software:

$$\begin{aligned}
 Y_1 = & 14.96 - 0.0003X_1 - 0.0021X_2 - 0.0487X_3 \\
 & - 0.0076X_4 + 0.0000X_1^2 + 0.0001X_2^2 + 0.0001X_3^2 \\
 & + 0.0001X_4^2 + 0.0000X_1X_2 - 0.0000X_1X_3 \\
 & + 0.0000X_1X_4 - 0.0000X_2X_3 + 0.0000X_2X_4 \\
 & + 0.0000X_3X_4
 \end{aligned} \quad (2)$$

$$\begin{aligned}
 Y_2 = & -64.41 + 0.0014X_1 + 0.0124X_2 - 0.2465X_3 \\
 & - 0.0379X_4 - 0.0000X_1^2 - 0.0005X_2^2 - 0.0002X_3^2 \\
 & - 0.0003X_4^2 - 0.0000X_1X_2 - 0.0000X_1X_3 \\
 & - 0.0000X_1X_4 + 0.0001X_2X_3 - 0.0000X_2X_4 \\
 & - 0.0000X_3X_4
 \end{aligned} \quad (3)$$

where Y_1 = band gap and Y_2 = PCE, X_1 = spin speed, X_2 = spin time, X_3 = annealing temperature and X_4 = annealing time.

The R^2 -adjusted value obtained for band gap is 99.35%, and for PCE it is 99.17%, which confirms that the accuracy and predictive ability of model is adequate. Additionally, the relationship between actual experimental values and predicted values is learned

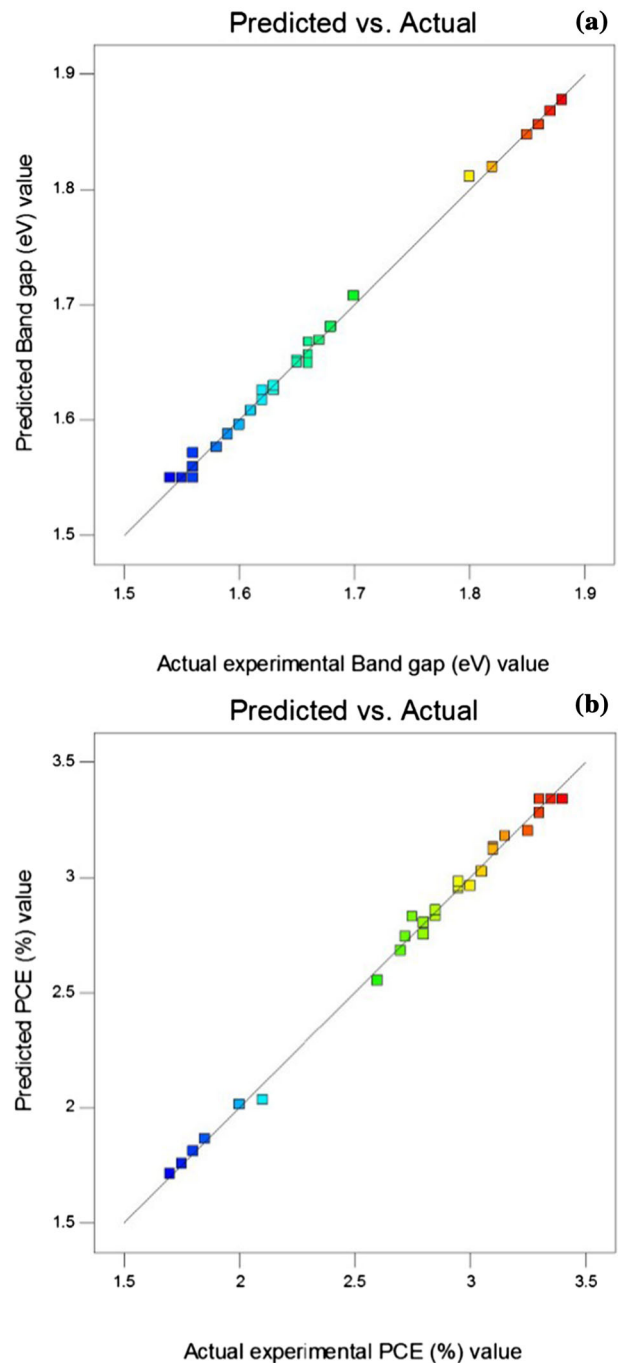


Figure 1 Scattered diagram of **a** actual experimental band gap of CZTS thin films versus predicted band gap of CZTS thin-film graph and **b** actual experimental PCE of CZTS thin-film-based solar cells versus predicted PCE of CZTS thin-film-based solar cells.

from the graph of actual versus predicted for both responses. Figure 1a and b depicts the actual versus predicted graph for band gap and PCE, respectively.

Furthermore, the effect of the control parameters on both the responses is determined by the analysis of variance (ANOVA). The ANOVA results of Table 2 obtained from software are depicted in Table 4. The most affecting parameter is decided based on the sum of square, *F* value and *p* value obtained in ANOVA results. The most affecting parameter should have a high sum of square value, high *F* value and low *p* value.

Influence of control parameters on the band gap and PCE

The band gap of CZTS thin film was obtained in the range of 1.54–1.88 eV for all 29 experiments. Based on Table 4, in the case of the band gap, the annealing temperature was the most significant parameter as indicated by high sum of square (0.200), high *F* value (2725.63) and low *p* value (< 0.0001). Subsequently, the second affecting parameter is annealing time (0.0070, 94.19 and < 0.0001, respectively). Spin speed is third affecting parameter. The least affecting parameter is spin time as compared to other parameters. Figure 2a depicts the effect of two most affecting parameters: annealing temperature and

annealing time on the band gap. Figure 2a clearly indicates that at low annealing temperature (450 °C), the band gap value is high as compared to generally reported 1.4–1.6 eV band gap for CZTS thin films [34–36]. These could be attributed to the presence of secondary phases at low temperature [18, 23, 37]. Upon increment in temperature (500 °C), the reduction in band gap was observed. However, further increment again caused the enlargement of the band gap. These could be attributed to the minor oxidation of CZTS thin films at high temperature. Similarly, band gap was reduced appropriately upon increasing annealing time from 30 to 60 min. Upon further increase in annealing time (90 min from 60 min), the band gap increases. These could be attributed to oxidation of film at high annealing time. Hence, the optimum value of annealing temperature would be in the range of 500–550 °C and annealing time would be 60–90 min.

It is well reported that the PCE is the function of the band gap. The optimum theoretical PCE of 33% is reported at around 1.45 eV band gap [38]. Hence, in the present study as well, band gap near to 1.5 produced superior PCE. In addition, the PCE is also dependent on the surface morphology. As both, void

Table 4 Analysis of variance (ANOVA) results for band gap and PCE model

Source	DF	SS		F value		p value	
		Band gap	PCE	Band gap	PCE	Band gap	PCE
Model	14	0.3200	7.7602	305.61	240.3169	< 0.0001	< 0.0001
A	1	0.0027	0.0675	36.29	29.2645	< 0.0001	< 0.0001
B	1	0.0019	0.0444	25.2	19.2533	0.0002	0.0006
C	1	0.2000	4.8133	2725.63	2086.8129	< 0.0001	< 0.0001
D	1	0.0070	0.1951	94.19	84.5745	< 0.0001	< 0.0001
AB	1	0.0000	0.6940	0	300.8596	1	< 0.0001
AC	1	0.0000	0.2425	0	105.1140	1	< 0.0001
AD	1	0.0001	2.2548	1.34	977.5466	0.2657	< 0.0001
BC	1	0.0004	0.3456	5.38	149.8457	0.0361	< 0.0001
BD	1	0.0000	0	0.34	0	0.5714	1.0000
CD	1	0.0000	0	0	0	1	1.0000
A ²	1	0.0280	0.0025	382.63	1.0839	< 0.0001	0.3155
B ²	1	0.0091	0.01	122.59	4.3355	< 0.0001	0.0562
C ²	1	0.0880	0.001225	1178.13	0.5311	< 0.0001	0.4782
D ²	1	0.0150	0	196.7	0	< 0.0001	1.0000
Residual	14	0.0010	0.03229				
Lack of fit	10	0.0006	0.02529	0.64	1.4452	0.741	0.3858
Pure error	4	0.0004	0.007				
Total	28	0.3200	7.7925				

DF degree of freedom, SS sum of squares

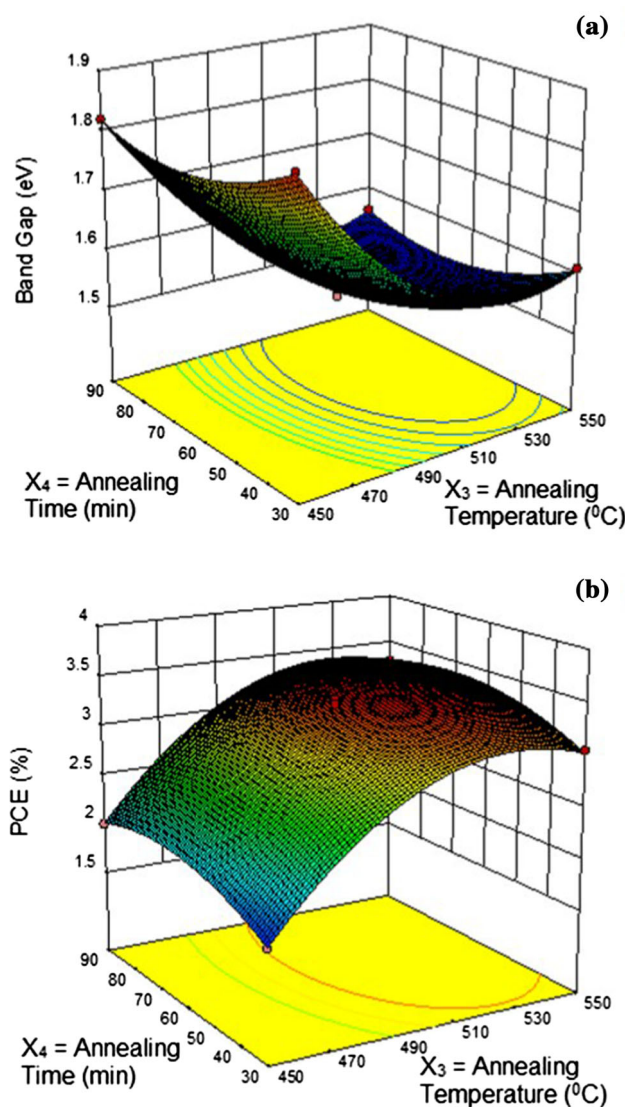


Figure 2 Three-dimensional (3D) response surface plot for influence of two most prominent affecting parameters (annealing temperature and annealing time) on the **a** band gap and **b** PCE.

and agglomeration of particle may adversely affect the PCE [24]. It is distinguished that surface morphology is the function of annealing temperature.

Hence, in the case of PCE the annealing temperature demonstrated a prominent effect ($SS = 4.81$, F value = 2086.81 and p value = < 0.0001) as in the case of band gap. Subsequently, annealing time and spin speed were second and third affecting parameters, respectively. Spin time seems to be insignificant as compared to other parameters ($SS = 0.044$, F value = 19.25 and p value = 0.0006) for PCE as in the case of band gap. Figure 2b depicts the effect of

two prominent control parameters, namely annealing temperature and annealing time on the CZTS thin-film-based solar cell PCE. From Fig. 2b, it is clear that similar to the band gap, low PCE is obtained at low annealing temperature (450 °C). Upon increment (500–550 °C) in the annealing temperature, PCE is increasing. Correspondingly, superior PCE is achieved at high annealing time (60–90 min) as compared to low annealing time (30 min).

Validation test

After, analyzing all the results and achieving a mathematical model, the model was optimized using optimization feature of the software. Consequently, a specific optimum condition, spin speed (X_1) = 2104 rpm, spin time (X_2) = 38 s, annealing temperature (X_3) = 527 °C and annealing time (X_4) = 68 min is achieved. The predictions of responses predicted for this optimum condition were 1.51 eV band gap and 3.53% PCE. Additionally, a validation test was carried out. Validation test was carried out at 2100 rpm spin speed, 38 s spin time, 530 °C annealing temperature and 68 min annealing time (nearest integer value). As a result, 1.50 eV band gap and 3.55% of PCE are achieved. The obtained results are very close to the prediction (1.51 eV band gap and 3.53% PCE). The achieved PCE is 17.55% higher than our previously reported (3.02%) [23]. Hence, it can be concluded that the models are perfectly fitted to both the responses and optimized well. The thickness of the optimum thin film was approximately 1 μm which is in range of commonly reported (1–2 μm) for CZTS thin film [3–5]. The Tauc's plot and XRD pattern of CZTS thin film prepared at optimum condition are depicted in Fig. 3. The band gap (see Fig. 3a) and XRD (see Fig. 3b) suggested that single-phase CZTS thin films were synthesized. XRD patterns confirm that typically reported kesterite structure of CZTS is present as (112) plane orientation is observed [39–41]. The surface morphology and cross-sectional SEM image of the thin film at three different locations are also shown in Fig. 3. The SEM images demonstrated uniform surface morphology (see Fig. 3c). Figure 3d depicts approximately 1 μm (873, 952 and 1100 nm) thickness of CZTS thin film. The J-V characteristics of the solar cell fabricated using CZTS thin film prepared at optimum condition are depicted in Fig. 4. The solar cell achieved 490 mV open-circuit voltage (V_{OC}), 14.5 mA cm^{-2} current

density (J_{SC}) and 50% fill factor (FF) and 3.55% of PCE which is 17.55% higher than our previously reported (3.02%) [21].

Conclusion

In the present study, CZTS thin films are prepared by sol-gel spin-coating method successfully. Further, the four major thin-film control parameters, namely spin speed (X_1), spin time (X_2), annealing temperature (X_3) and annealing time (X_4), are investigated. Subsequently, the optimization of the control parameter in terms of multiple responses (band gap and PCE) is successfully carried out for the first time for sol-gel spin-coated CZTS thin films. The RSM method, Box-Behnken design array is implemented for the optimization. Additionally, the influence of the control parameters on both band gap and PCE is observed by analysis of variance (ANOVA) results. In both the

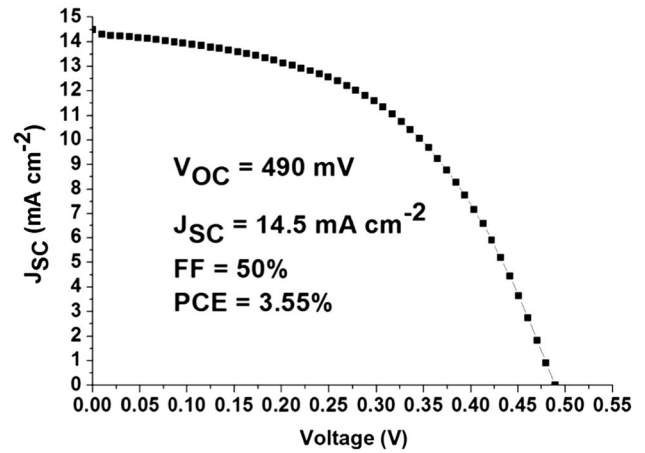


Figure 4 J-V characteristics of the solar cell fabricated using the CZTS thin film prepared at optimum deposition condition.

cases, annealing temperature is observed to be the major control parameter. The second prominent control parameter is annealing time, and spin speed is observed to be third. In comparison with other

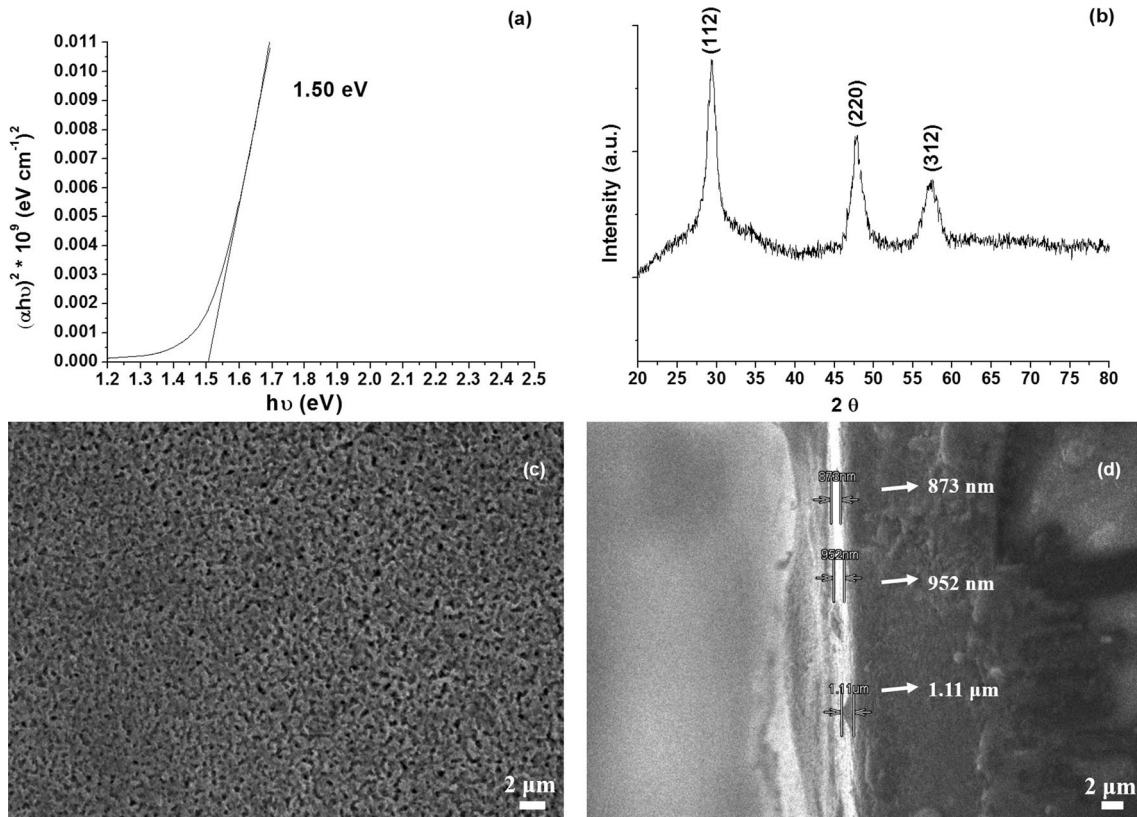


Figure 3 **a** Tauc's plot, **b** XRD pattern, **c** surface morphology and **d** cross-sectional SEM image of the CZTS thin film prepared at optimum deposition condition.

three parameters, the spin time is proved to be insignificant in both the cases. Furthermore, the mathematical quadratic models are developed for both the responses as the function of control parameters. Moreover, the obtained models are optimized by the help of Design Expert software. Specific optimum condition spin speed (X_1) = 2104 rpm, spin time (X_2) = 38 s, annealing temperature (X_3) = 527 °C and annealing time (X_4) = 68 min is obtained. 1.51 eV band and 3.53% PCE are mathematically predicted for the obtained specific condition. In addition, a validation test is carried out, and as a result, 1.50 eV band gap and 3.55% PCE are achieved. These results suggested that both the models are appropriately fitting and optimized well. The achieved PCE is 17.55% higher than our previously reported PCE. The acquired optimum condition can be further applied in other solar cells to ease further improvement in PCE.

Funding

This study was not funded by any grant.

Compliance with ethical standards

Conflict of interest The authors declare that we have no conflict of interest.

References

- [1] Singh GK (2013) Solar power generation by PV (photo-voltaic) technology: a review. *Energy* 53:1–13
- [2] Green MA, Emery K, Hishikawa Y et al (2017) Solar cell efficiency tables (version 49): solar cell efficiency tables (version 49). *Prog Photovolt Res Appl* 25:3–13
- [3] Conibeer G, Green M, Corkish R et al (2006) Silicon nanostructures for third generation photovoltaic solar cells. *Thin Solid Films* 511–512:654–662
- [4] Yan J, Saunders BR (2014) Third-generation solar cells: a review and comparison of polymer:fullerene, hybrid polymer and perovskite solar cells. *RSC Adv* 4:43286–43314
- [5] Suryawanshi MP, Agawane GL, Bhosale SM et al (2013) CZTS based thin film solar cells: a status review. *Mater Technol* 28:98–109
- [6] Romanyuk YE, Fella CM, Uhl AR et al (2013) Recent trends in direct solution coating of kesterite absorber layers in solar cells. *Sol Energy Mater Sol Cells* 119:181–189
- [7] Patel SB, Gohel JV (2018) Recent developments in $\text{Cu}_2\text{ZnSnS}_4$ (CZTS) preparation, optimization and its application in solar cell development and photocatalytic applications. In: Tayade RJ, Gandhi V (eds) *Photocatalytic nanomaterials for environmental applications*. Materials Research Forum LLC, Millersville, pp 370–404
- [8] Sripan C, Madhavan VE, Viswanath AK, Ganesan R (2017) Sulfurization and annealing effects on thermally evaporated CZTS films. *Mater Lett* 189:110–113
- [9] Li X, Su Z, Venkataraj S et al (2016) 8.6% Efficiency CZTSSe solar cell with atomic layer deposited Zn–Sn–O buffer layer. *Sol Energy Mater Sol Cells* 157:101–107
- [10] Shin S, Park C, Kim C et al (2016) Cyclic voltammetry studies of copper, tin and zinc electrodeposition in a citrate complex system for CZTS solar cell application. *Curr Appl Phys* 16:207–210
- [11] Patel SB, Gohel JV (2018) Enhanced solar cell performance by optimization of spray coated CZTS thin film using Taguchi and Response Surface Method. *J Mater Sci Mater Electron* 29:5613–5623. <https://doi.org/10.1007/s10854-018-8530-5>
- [12] Orletsyky IG, Solovan MM, Brus VV et al (2017) Structural, optical and electrical properties of $\text{Cu}_2\text{ZnSnS}_4$ films prepared from a non-toxic DMSO-based sol–gel and synthesized in low vacuum. *J Phys Chem Solids* 100:154–160
- [13] Ghorpade U, Suryawanshi M, Shin SW et al (2014) Towards environmentally benign approaches for the synthesis of CZTSSe nanocrystals by a hot injection method: a status review. *Chem Commun* 50:11258–11273
- [14] Yu Y, Ge J, Prabhakar T, Yan Y (2014) Effects of spin speed on the properties of spin-coated $\text{Cu}_2\text{ZnSnS}_4$ thin films and solar cells based on DMSO solution. In: 2014 IEEE 40th Photovolt Spec Conf PVSC 2014, pp. 448–451
- [15] Wu Q, Xue C, Li Y et al (2015) Kesterite $\text{Cu}_2\text{ZnSnS}_4$ as a low-cost inorganic hole-transporting material for high-efficiency perovskite solar cells. *ACS Appl Mater Interfaces* 7:28466–28473
- [16] Agawane GL, Kamble AS, Vanalakar SA et al (2015) Fabrication of 3.01% power conversion efficient high-quality CZTS thin film solar cells by a green and simple sol-gel technique. *Mater Lett* 158:58–61
- [17] Nguyen TH, Septina W, Fujikawa S et al (2015) $\text{Cu}_2\text{ZnSnS}_4$ thin film solar cells with 5.8% conversion efficiency obtained by a facile spray pyrolysis technique. *RSC Adv* 5:77565–77571
- [18] Prabeesh P, Selvam IP, Potty SN (2016) Effect of annealing temperature on a single step processed $\text{Cu}_2\text{ZnSnS}_4$ thin film via solution method. *Thin Solid Films* 606:94–98
- [19] Tchognia JHN, Arba Y, Hartiti B et al (2016) Effect of sulfurization time on properties of $\text{Cu}_2\text{ZnSnS}_4$ thin films

- obtained by sol–gel deposited precursors. *Opt Quantum Electron* 48:1–7
- [20] Nkuisi Tchognia JH, Hartiti B, Ridah A et al (2016) Application of Taguchi approach to optimize the sol-gel process of the quaternary $\text{Cu}_2\text{ZnSnS}_4$ with good optical properties. *Opt Mater (Amst)* 57:85–92
- [21] Wei XL, Xia Y, Liu XM et al (2014) Preparation of sodium beta γ -alumina electrolyte thin film by electrophoretic deposition using Taguchi experimental design approach. *Electrochim Acta* 136:250–256
- [22] Izuan J, Rashid A, Yusof NA, Abdullah J (2016) Surface modifications to boost sensitivities of electrochemical biosensors using gold nanoparticles/silicon nanowires and response surface methodology approach. *J Mater Sci* 51:1083–1097. <https://doi.org/10.1007/s10853-015-9438-6>
- [23] Patel S, Gohel JV (2017) Effect of annealing atmosphere and temperature on the properties of the sol-gel spin coated $\text{Cu}_2\text{ZnSnS}_4$ (CZTS) thin films. *Int J Res* 4:970–974. <https://edupediapublications.org/journals/index.php/IJR/article/view/9331>
- [24] Patel SB, Gohel JV (2017) Effect of type of solvent on the sol–gel spin coated CZTS thin films. *Phys Astron Int J* 1:1–5. <https://doi.org/10.15406/paij.2017.01.00023>
- [25] Kumari N, Gohel JV, Patel SR (2017) Multi-response optimization of ZnO thin films using Grey-Taguchi technique and development of a model using ANN. *Opt Int J Light Electron Opt* 144:422–435
- [26] Gohel JV, Jana AK, Singh M (2017) Highly enhanced photocurrent of novel quantum-dot-co-sensitized PbS–Hg/CdS/Cu: ZnO thin films for photoelectrochemical applications. *Appl Phys A* 123:1–12
- [27] Lanjewar M, Gohel JV (2017) Enhanced performance of Ag-doped ZnO and pure ZnO thin films DSSCs prepared by sol-gel spin coating. *Inorg Nano-Metal Chem* 47:1090–1096
- [28] Box GEP, Draper NR (1987) Empirical model-building and response surfaces. Wiley Ser Probab Math, Stat, p 669
- [29] Jagadish PR, Khalid M (2017) Process optimisation for n-type Bi_2Te_3 films electrodeposited on flexible recycled carbon fibre using response surface methodology. *J Mater Sci* 52:11467–11481. <https://doi.org/10.1007/s10853-017-1284-2>
- [30] Venter JC, Smith HO, Hood L (1996) A new strategy for genome sequencing. *Nature* 381:364–366
- [31] Swami SK, Kumar A, Dutta V (2013) Deposition of kesterite $\text{Cu}_2\text{ZnSnS}_4$ (CZTS) thin films by spin coating technique for solar cell application. *Energy Procedia* 33:198–202
- [32] Wang J, Zhang P, Song X, Gao L (2014) $\text{Cu}_2\text{ZnSnS}_4$ thin films: spin coating synthesis and photoelectrochemistry. *RSC Adv* 4:21318–21324
- [33] Liu R, Tan M, Zhang X et al (2016) Impact of sol-gel precursor treatment with preheating temperature on properties of $\text{Cu}_2\text{ZnSnS}_4$ thin film and its photovoltaic solar cell. *J Alloys Compd* 655:124–129
- [34] Henry J, Mohanraj K, Sivakumar G (2016) Electrical and optical properties of CZTS thin films prepared by SILAR method. *J Asian Ceram Soc* 4:81–84
- [35] Thiruvenkadam S, Jovina D, Leo Rajesh A (2014) The influence of deposition temperature in the photovoltaic properties of spray deposited CZTS thin films. *Sol Energy* 106:166–170
- [36] Mokurula K, Mallick S, Bhargava P (2014) Low temperature synthesis and characterization of $\text{Cu}_2\text{ZnSnS}_4$ (CZTS) nanoparticle by solution based solid state reaction Method. *Energy Procedia* 57:73–78
- [37] Hosseinpour R, Izadifard M, Ghazi ME, Bahramian B (2017) Effect of annealing temperature on structural, optical, and electrical properties of sol-gel spin-coating-derived $\text{Cu}_2\text{ZnSnS}_4$ thin films. *J Electron Mater* 47:1080–1090
- [38] Shockley W, Queisser HJ (1961) Detailed balance limit of efficiency of p-n junction solar cells. *J Appl Phys* 32:510–519
- [39] Khalil MI, Atici O, Lucotti A et al (2016) CZTS absorber layer for thin film solar cells from electrodeposited metallic stacked precursors (Zn/Cu-Sn). *Appl Surf Sci* 379:91–97
- [40] Pang Z, Wei A, Zhao Y et al (2018) materials Direct growth of $\text{Cu}_2\text{ZnSnS}_4$ on three-dimensional porous reduced graphene oxide thin films as counter electrode with high conductivity and excellent catalytic activity for dye-sensitized solar cells. *J Mater Sci* 53:2748–2757. <https://doi.org/10.1007/s10853-017-1741-y>
- [41] Al-shakban M, Matthews PD, Savjani N et al (2017) The synthesis and characterization of $\text{Cu}_2\text{ZnSnS}_4$ thin films from melt reactions using xanthate precursors. *J Mater Sci* 52:12761–12771. <https://doi.org/10.1007/s10853-017-1367-0>